Available online at www.sciencedirect.com
ScienceDirect
International Journal of Heat and Mass Transfer 50 (2007) 2272–2281
International Journal of HEAT and MASS TRANSFER
www.elsevier.com/locate/ijhmt

Heat transfer and flow behaviour of aqueous suspensions of TiO_2 nanoparticles (nanofluids) flowing upward through a vertical pipe

Yurong He [a], Yi Jin [b], Haisheng Chen [c], Yulong Ding [a,*], Daqiang Cang [b], Huilin Lu [d]

[a] Institute of Particle Science and Engineering, University of Leeds, Leeds LS2 9JT, UK
[b] Institute of Environmental Engineering, University of Science and Technology, Beijing, China
[c] Institute of Engineering Thermophysics, Chinese Academy of Sciences, Beijing, China
[d] Institute of Thermal Power Engineering, Harbin Institute of Technology, Harbin, China

Received 5 May 2006
Available online 18 December 2006

Abstract

Stable aqueous TiO_2 nanofluids with different particle (agglomerate) sizes and concentrations are formulated and measured for their static thermal conductivity and rheological behaviour. The nanofluids are then measured for their heat transfer and flow behaviour upon flowing upward through a vertical pipe in both the laminar and turbulent flow regimes. Addition of nanoparticles into the base liquid enhances the thermal conduction and the enhancement increases with increasing particle concentration and decreasing particle (agglomerate) size. Rheological measurements show that the shear viscosity of nanofluids decreases first with increasing shear rate (the shear thinning behaviour), and then approaches a constant at a shear rate greater than $\sim 100\ s^{-1}$. The constant viscosity increases with increasing particle (agglomerate) size and particle concentration. Given the flow Reynolds number and particle size, the convective heat transfer coefficient increases with nanoparticle concentration in both the laminar and turbulent flow regimes and the effect of particle concentration seems to be more considerable in the turbulent flow regime. Given the particle concentration and flow Reynolds number, the convective heat transfer coefficient does not seem to be sensitive to the average particle size under the conditions of this work. The results also show that the pressure drop of the nanofluid flows is very close to that of the base liquid flows for a given Reynolds number.

Keywords: Nanofluids; Convective heat transfer; TiO_2 nanoparticles; Thermal conductivity; Viscosity; Pressure drop; Mechanism; Effect of nanoparticle size

1. Introduction

A heat transfer fluid is a fluid medium used in a system for adding to or removing from the system an amount of heat at an adequate rate to ensure the functionality and reliability of the system. The efficacy of such a fluid depends on both the physical properties of the fluid including thermal conductivity, viscosity, density, and heat capacity, and its interaction with the environment where heat is to be transferred. Examples of heat transfer fluids include water, minerals oil and ethylene glycol, which have been widely used for many decades in various industrial sectors (e.g. power generation, chemical production, transportation and microelectronics), and offices and homes (e.g. refrigeration, air conditioning and central heating). These conventional heat transfer fluids, however, are often limited by their poor thermal properties in particular thermal conductivity, which implies bulky heat exchangers and high pumping power.

Driven by industrial needs of process intensification and device miniaturization, development of high performance heat transfer fluids has been a subject of numerous investigations in the past few decades. As solids materials in particular metals can have very high thermal conductivities,

* Corresponding author. Tel.: +44 113 343 2747; fax: +44 113 343 2405.
E-mail address: y.ding@leeds.ac.uk (Y. Ding).

0017-9310/$ - see front matter © 2006 Elsevier Ltd. All rights reserved.
doi:10.1016/j.ijheatmasstransfer.2006.10.024

Nomenclature

a	thermal diffusivity	S	perimeter of the test tube
A	cross-sectional area of the test section	T_{ave}	average temperature
c	heat capacity of fluid	T_f	fluid temperature
D	test tube inner diameter	T_{in}	fluids inlet temperature
f	friction factor	T_w	wall temperature
h	convective heat transfer coefficient	u	fluid velocity
k_f	thermal conductivity of the fluid	x	axial position
k_l	thermal conductivity of the base liquid		
k_p	solids phase thermal conductivity	*Greek symbols*	
L	tube length	ρ_f	fluids density
n	shape factor	μ_f	fluids viscosity
Nu	Nusselt number	μ_l	base fluid viscosity
Pr	Prandtl number	ν	fluid kinematic viscosity
Δp	pressure drop	ϕ	particle volume fraction
q	heat flux	ψ	sphericity
Re	Reynolds number	δ_t	boundary layer thickness

lots of studies have been carried out in the past on the thermal behaviour of suspensions of particulate solids in liquids; see for example [25,1,2,12]. These early studies, however, used suspensions of millimeter or micrometer sized particles, which, although showed some enhancement, experienced problems such as abrasion and channel clogging due to poor suspension stability. The channel clogging can be particularly serious for systems using mini- and/or micro-channels. A recent invention termed 'nanofluids' has shown potential to resolve some disadvantages associated with suspensions of large particles [3]. Nanofluids are liquid suspensions containing particles that are significantly smaller than 100 nm in at least one dimension, and have bulk thermal conductivities orders of magnitudes higher than the base liquids. The potential advantages of properly engineered nanofluids include (a) higher thermal conductivities than that predicted by currently available macroscopic models, (b) excellent stability, and (c) little penalty due to an increase in pressure drop and pipe wall abrasion experienced by suspensions of millimeter or micrometer particles. As a result of these potential advantages, a number of studies have been performed on the thermal properties of nanofluids since the invention approximately a decade ago; see for examples [20,3,8,27,17,34,9,14,32,36,28,29,18,7]. These studies are mostly on the effective thermal conductivity under macroscopically static conditions, and only small number of studies have been carried out on the other aspects such as phase change behaviour [4–6,38,26,30]) and convective heat transfer [16,22,33,19,35,15,29,31,37,7].

This work is concerned about the forced convective heat transfer of aqueous suspensions of titanium dioxide nanoparticles (TiO_2 nanofluids). The reasons for choosing TiO_2 include (a) TiO_2 is generally regarded as safe material for human being and animals (they are actually used in the cosmetic products, and water treatment), (b) TiO_2 nanoparticles are easily obtained (they are produced in very large industrial scales), (c) TiO_2 nanofluids have an excellent stability even without using any stabilizer and (d) metal oxides such TiO_2 nanoparticles are chemically more stable than their metallic counterparts.

Stable TiO_2 nanofluids are formulated and characterized followed by experiments on the flow and heat transfer behaviour of the nanofluids flowing upwards in a straight pipe under both laminar and turbulence/transition conditions. The motivations behind are: (a) little is found in the literature on the convective heat transfer of TiO_2 nanofluids; (b) most reported studies on the convective heat transfer of nanofluids did not include full information of nanofluid formulation and characterization, which makes it difficult to compare the results from these studies; (c) little is found in the literature on the effect of particle (agglomerate) size on the convective heat transfer performance; and (d) there are inconsistencies in the few reported studies on the convective heat transfer using nanofluids [22,35,37,29,7].

2. Experimental

2.1. Materials and nanofluids formulation

Dry titanium dioxide nanoparticles and distilled water were used to prepare nanofluids. The nanoparticles was purchased from Degussa (Germany) and used as received. X-ray diffraction analysis showed the nanoparticles contained dominantly anatase phase with a small amount of rutile phase. Fig. 1 shows an SEM image of the sample. It can be seen that the primary nanoparticles are approximately spherical with an average diameter of about 20 nm.

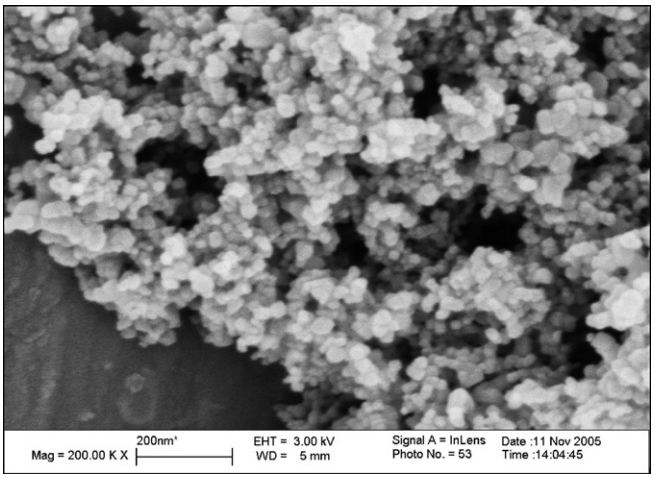

Fig. 1. An SEM micrograph of the TiO_2 nanoparticles.

However, the dry nanoparticles are in the form of large agglomerates. In order to break down the large agglomerates, ultrasonication was applied for 30 min to mix a preset amount of nanoparticles with water to give certain nanoparticle concentration. The suspension was then processed in a medium-mill to reduce the agglomerate size further (Dyno Multi-Lab Mill, Willy A. Bachofen of Switzerland). As no stabiliser was used in this work, the pH value of the suspension was adjusted to 11 to prevent re-agglomeration of the milled samples. Such a pH level gave a high zeta-potential of the particles of ~ -40 mV. Note that the test section is made of copper as will be described in Section 2.3. Copper has a very low iso-electric point [13], which gave a zeta potential of ~ -45 mV at pH = 11. This prevented deposition of TiO_2 nanoparticles and possible subsequent fouling the copper tube.

A Malvern nanosizer (Malvern Instrument, UK) was used to measure the particle size distribution of the suspension processed for different lengths of time. The average size of particles in the suspension was $\sim$500 nm after $\sim$30 min sonication. Processing of the suspension in the Dyno-mill led to a rapid decrease in the particle size to $\sim$120 nm in the first 30 min. However, further processing of the suspension with the mill was not effective. For example, further processing for several hours only gave an average particle size of $\sim$95 nm.

Nanofluids containing 1.0%, 2.5%, 4.9% TiO_2 particles by weight were produced by using the methods as described above. The three weight concentrations corresponded approximately to 0.24%, 0.60% and 1.18% by volume (the density of TiO_2 was taken as 4170 kg/m^3). For the 2.5 wt% (0.6 vol.%) TiO_2 nanofluids, three average particle sizes of 95 nm, 145 nm and 210 nm were obtained by using different processing durations. Note that the sizes given here are hydrodynamic diameters of aggregates of nanoparticles. They are less dense than the primary nanoparticles. The nanofluids thus obtained were found to be very stable for months.

2.2. Measurements of the effective thermal conductivity and viscosity of TiO_2 nanofluids

Quantitative evaluation of the convective heat transfer behaviour of nanofluids requires the effective thermal conductivity and viscosity. The thermal conductivity was measured by using a KD2 thermal property meter (Labcell Ltd., UK). The KD2 meter is based on the well-known hot-wire method, which has a probe with 60 mm length and 0.9 mm diameter. The probe integrates in its interior a heating element and a thermo-resistor, and is connected to a microprocessor for controlling and conducting the measurements. The KD2 meter was calibrated by using distilled water before any set of measurements. Nanofluids samples were held in cylindrical glass containers with 35 mm diameter and 80 mm height. The glass containers were located in a thermostat bath (GD120-S12, Grant, UK) set at 22 °C to ensure all the measurements at a constant temperature. The thermostat was able to maintain the temperature uniformity within $\pm$0.02 K. At least five measurements were taken for each nanofluid sample to ensure the uncertainty of the measurements within 3%.

The viscosity of nanofluids was measured by using a Bohlin CVO rheometer with a Mooney cell (Malvern Instruments, UK). The measurements were done at 22 °C on the nanofluids of different concentrations and containing particles of the three different sizes.

2.3. Measurements of the convective heat transfer coefficient and pressure drop

The experimental system for measuring the convective heat transfer coefficient and pressure drop is shown schematically in Fig. 2. It consisted of a flow loop, a heating unit, a cooling unit, and a measuring and control unit. The flow loop included a pump with a built-in flowmeter, a nanofluid tank, a collection tank, a test section and

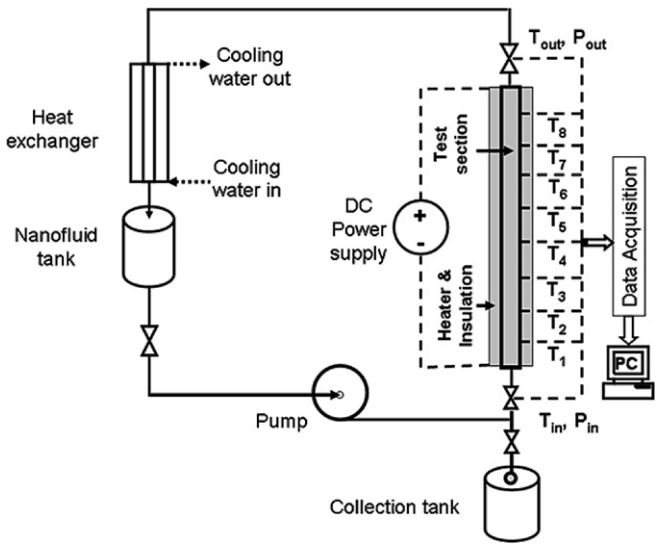

Fig. 2. Experimental system.

various valves. The test section was a vertically oriented straight copper tube with 1834 mm length, 3.97 mm inner diameter, and 6.35 mm outer diameter. The tube was heated by two flexible silicon rubber heaters (Watlow, UK) linked to a DC power supply (TTi Ex752 m, RS, UK). The power supply was adjustable and had a maximum power supply of 300 W. There was a thick thermal isolating layer surrounding the heaters to obtain a constant heat flux condition along the test section. Eight T-type thermocouples were mounted on the test section at the normalised axial positions with respect to the tube inner diameter of ~50.4 (T1), 151.2 (T2), 201.6 (T3), 252.0 (T4), 302.4 (T5), 352.8 (T6), 403.2 (T7) and 453.6 (T8) from the inlet of the test section to measure the wall temperature distribution. Two further T-type thermocouples were inserted into the flow at the inlet and exit of the test section to measure the bulk temperatures of nanofluids. Two pressure transducers (RS 286-686, RS, UK) were installed at the inlet and outlet of the test section to measure the pressure drop. The pump used in this work was of peristaltic type with the flowrate controlled by the rotational rate. The maximum flow rate the pump could deliver was 10 l per minute. Nanofluids were driven by the pump to flow upward through the test section. A tube-in-shell type heat exchanger was used to cool the nanofluids to help with reaching the steady state, where laboratory cooling water was used as the coolant. There was a three-way valve in the flow loop for flowrate calibrations and flow system cleaning between runs even with the same nanofluid. In the heat transfer experiments, the pump rotational rate, voltage and current of the DC power supply were recorded and the temperature readings from the 10 thermocouples and two pressure transducers were registered by a data requisition system (DAQ, National Instrument, UK). As the pump performance was sensitive to the fluid viscosity at a given rotational speed, calibration was needed, which was carried out before and after each experiment by a weighing method. This gave an accuracy of nanofluids flowrate better than 5%. The thermocouples were calibrated in a thermostat water bath and the accuracy was found to be within ±0.1 K.

The convective heat transfer coefficient (h) is defined as

$$h(x) = q/(T_w(x) - T_f(x)) \quad (1)$$

where x represents axial distance from the entrance of the test section, q is the heat flux, T_w is the measured wall temperature, and T_f is the fluid temperature decided by the following energy balance equation:

$$T_f(x) = T_{in} + qSx/(\rho_f cuA) \quad (2)$$

where c is the heat capacity, ρ_f is the fluid density, A and S are respectively the cross-sectional area and perimeter of the test tube, and u is the average fluid velocity. Eq. (2) is based on an assumption of zero heat loss through the insulation layer. The deviation to this assumption was assessed by comparing the measured temperature difference between the inlet and outlet of the test section with the theoretical value calculated by Eq. (2). It was found that the maximum deviation was lower than 6.5% under the conditions of this work.

The convective heat transfer coefficient, h, in Eq. (1) is usually expressed in the form of the Nusselt number (Nu) as

$$Nu(x) = h(x)D/k_f \quad (3)$$

where D is the tube inner diameter, and k_f is the fluid thermal conductivity. Traditionally, the Nu number is related to the Reynolds number defined as $Re = \rho_f uD/\mu_f$ and the Prandtl number defined as $Pr = v/a$, where v is the fluid kinematic viscosity, a is the fluid thermal diffusivity, and μ_f is the fluid dynamic viscosity.

3. Results and discussion

3.1. The thermal conductivity of nanofluids

Fig. 3(a) shows the measured effective thermal conductivity of TiO_2 nanofluids as a function of particle concentration. Also included in the figure are the data reported by Murshed et al. [21] and the prediction by the following

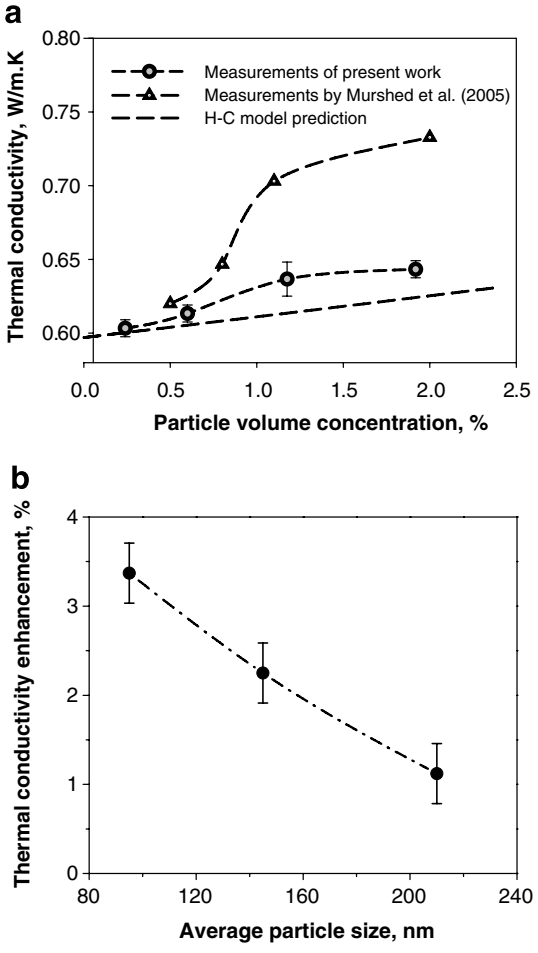

Fig. 3. Effects of (a) particle concentration (95 nm particles) and (b) size (0.6% by volume) on the thermal conductivity of aqueous TiO_2 nanofluids.

conventional H–C model for particles uniformly dispersed in a continuum medium [11]

$$k_f = k_l\left[\frac{k_p + (n-1)k_l - (n-1)\phi(k_l - k_p)}{k_p + (n-1)k_l + \phi(k_l - k_p)}\right] \quad (4)$$

where n is the shape factor given by $n = 3/\psi$ with ψ the sphericity ($\psi = 1$ for spherical particles). k_l and k_p are the thermal conductivities of the base fluid and particles, respectively. It can be seen that the measured effective thermal conductivity of nanofluids increases with increasing nanoparticle concentration in a non-linear fashion, which differs from the H–C model prediction in two aspects: the predicted thermal conductivity is much lower than the measured values and prediction shows linear dependence on the particle concentration. The measured non-linear dependence agrees well with the results reported by Murshed et al. [21] although there is a significant difference between the two sets of experimental results, particularly at high particle concentrations. The exact reasons for the considerable difference is unclear but different nanoparticle sizes and solution chemistry (e.g. pH) used in the two studies could be possible reasons.

Fig. 3(b) shows the effect of particle size on the effective nanofluids thermal conductivity where the data have been processed to give the enhancement with respect to the thermal conductivity of the base liquid under the same conditions. It is clearly shown that the effective thermal conductivity decreases with particle (aggregate) size. This has actually observed recently by Lee et al. [18] who measured the effective thermal conductivity of aqueous based CuO nanofluids with different aggregate sizes obtained by changing the pH levels.

A further inspection of Fig. 3(a) and (b) shows the non-linear dependence of the effective thermal conductivity of nanofluids on both particle concentration and size and the non-linearity is more considerable in terms of the effect of particle concentration. The exact reason is unclear but is believed to be associated with nanoparticle structuring that increases with increasing particle concentration. Further investigation is clearly needed.

A number of studies have been published on the mechanisms of thermal conduction enhancement. This will not be discussed further here as the main focus is on heat transfer of flowing nanofluids. For those who are interested in finding more please refer to Keblinski et al. [14], Wen and Ding [28], and Lee et al. [18].

3.2. The viscosity of nanofluids

Rheological measurements show that the TiO_2 nanofluids are shear thinning over the shear rate range of 0.1 and 1000 1/s tested in this work. Fig. 4(a) shows an example of the shear viscosity as a function of shear rate for 1.18 vol.% 95 nm TiO_2 nanofluid. The results under other conditions are similar. One can see that the shear viscosity decreases rapidly with increasing shear rate until the shear rate reaches ~100 1/s above which a constant shear viscosity is observed. If the constant shear viscosity is plotted against the particle concentration and average particle size, Fig. 4(b) and (c) are obtained. One can see that the shear viscosity increases with increasing TiO_2 concentration given the particle size, and given the particle concentration, the shear viscosity increases with increasing particle size. Shown in Fig. 4(b) also includes the prediction by the Einstein equation, $\mu_f = \mu_l(1 + 2.5\phi)$, for non-interacting dilute suspensions of particles, where μ_l is the base liquid

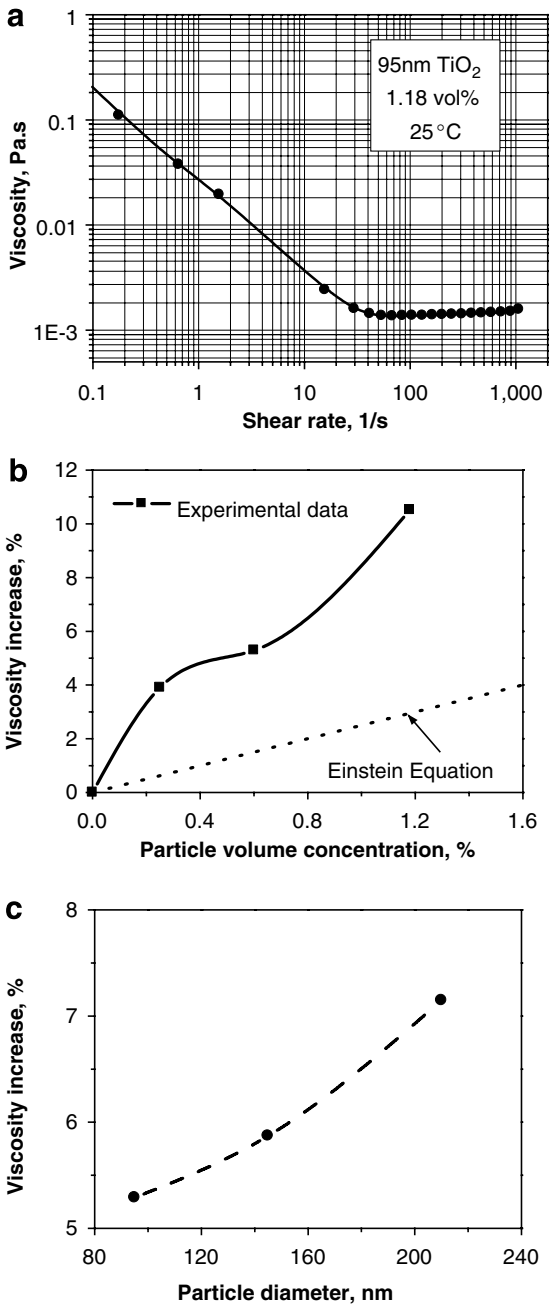

Fig. 4. Effects of shear rate, particle concentration and size on the nanofluids viscosity. (a) Viscosity of nanofluids as a function of shear rate, (b) effect of particle concentration (95 nm) and (c) effect of particle size (0.6%).

viscosity. Two observations can be made from the figure. First, the measured viscosity of nanofluids is much higher than that predicted by the Einstein equation, indicating strong interactions between particles in the nanofluids. Second, the measured nanofluid viscosity relates to the particle volume concentration in a non-linear fashion. The exact reason for the non-linearity requires further investigations but different structures of nanofluids at different concentrations may be a possible reason. Pak and Cho [22] measured the viscosity of aqueous suspensions of titanium oxide nanoparticles with a mean diameter of 27 nm and found an increases in the viscosity by ~12% at a volume concentration of 0.99%, which is higher than that obtained in this work possibly due to stronger interactions between smaller nanoparticles used in their work.

A further inspection of Fig. 4(b) and (c) shows that the non-linearity of the dependence of the viscosity on particle concentration is more considerable than that on particle size. This is similar to the case for the effective thermal conductivity as discussed in Section 3.1. Such a coincidence seems to suggest existence of a relationship between the two effective transport properties of nanofluids, which clearly requires further investigation.

3.3. Convective heat transfer

3.3.1. Convective heat transfer coefficient of pure water

Before systematic experiments were performed on TiO_2 nanofluids, the experimental system was tested with pure water adjusted to a pH value of 11 as the working fluid. The results with the pure water will also serve as the basis for comparison with the results of nanofluids. Fig. 5(a) and (b) show the pure water results in the laminar flow regime ($Re < 2300$) at two Reynolds numbers of $Re = 900$ and 1500, and in the turbulence/transition regime ($Re > 2300$) at a Reynolds number of $Re = 4800$. Also shown are predictions with the following Shah equation for the laminar flows [23] and Gnielinski equation [10] for the turbulent flows under the constant heat flux boundary conditions:

Shah equation for laminar flows:

$$Nu = \begin{cases} 1.953\left(RePr\frac{D}{x}\right)^{1/3} & \left(RePr\frac{D}{x}\right) \geqslant 33.3 \\ 4.364 + 0.0722RePr\frac{D}{x} & \left(RePr\frac{D}{x}\right) < 33.3 \end{cases} \quad (5)$$

Gnielinski equation for turbulent flows:

$$Nu = \frac{(f/2)(Re - 10^3)Pr}{1 + 12.7(f/2)^{1/2}(Pr^{2/3} - 1)} \quad (6)$$

The Nusselt number in Eqs. (5) and (6) has been defined by Eq. (3). The local convective heat transfer coefficient, h, used to calculate the Nusselt number is given by $h = -k_f(\partial T/\partial r)_w/(T_w - T_{ave})$ with $(\partial T/\partial r)_w$ the radial temperature gradient at the wall, and T_w and T_{ave} respectively the wall temperature and average temperature across the tube cross-section at a given axial position. f in Eq. (6) is the friction factor given by

$$f \cong 0.078Re^{-1/4} \quad (6a)$$

Eq. (6) has been shown to be accurate within ±10% in the range of $0.5 < Pr < 10^6$ and $2300 < Re < 5 \times 10^6$. Note that Eq. (6) does not include the effect of the entrance, which is expected to be small for turbulent flows as will be discussed further in the following.

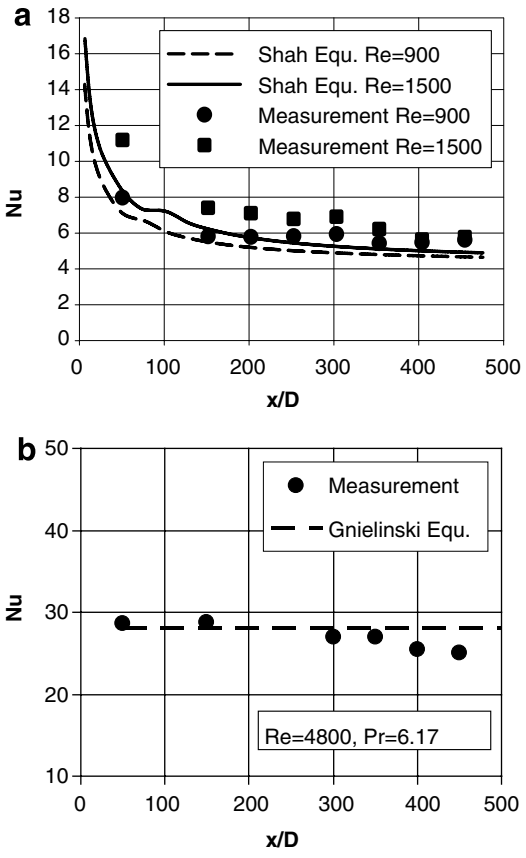

Fig. 5. Comparison of the measurements with the empirical Shah and Gnielinski equations for pure water flows. (a) Laminar flows and (b) turbulent flows.

An inspection of Fig. 5(a) shows that the Shah equation slightly underpredicts the measurements in the laminar flow regime. This is likely to be associated with the relatively high pH condition used in this work, which may change the interfacial wetting conditions hence the convective heat transfer. (The effect of pH condition seems to impose little effect on the heat transfer under turbulent conditions; see below.) The small bumps in predicted curves by the Shah equation are because the empirical expression consists of two parts demarcated by $RePr(D/x) = 33.3$.

In the turbulent regime, the Gnielinski equation predicts very well the measurements over the whole range of x/D. The experimental results shown in Fig. 5(b) also indicate little effect of the entrance length on the heat transfer in the turbulent flow regime.

Having built-up the confidence in the experimental system, systematic experiments were performed on nanofluids

under various conditions. The results are presented and discussed in the following sub-sections.

3.3.2. Effect of nanoparticle concentrations on the convective heat transfer

Fig. 6(a) and (b) shows the axial profiles of the heat transfer coefficient of nanofluids with different particle concentrations in the laminar and turbulent flow regimes, respectively. The Reynolds number given in the figures is based on the viscosity of the base liquid hence the same Reynolds number indicates approximately the same fluid velocity due to very low particle concentrations in the nanofluids. Enhancement of the convective heat transfer coefficient is observed in both the laminar and turbulent flow regimes and the enhancement increases with increasing particle concentration. The enhancement in the laminar flow regime is much smaller than that in the turbulent flow regime. For example, at $Re = 1500$, the maximum enhancement with 1.1 vol.% TiO_2 nanofluids is about 12%, whereas at $Re = 5900$, the maximum enhancement with the same 1.1 vol.% TiO_2 nanofluids exceeds 40%.

As mentioned above, the above analyses are based on the Reynolds numbers calculated by using the viscosity of the base liquid. It would be more meaningful if the Reynolds number is calculated based on the value of nanofluid viscosity taking into account of the shear rate dependence as discussed in Section 3.2. Fig. 7(a) and (b) shows the results for $x/D = 151$. Enhancement is clearly seen for both laminar and turbulent flow regimes and the enhancement increases with increasing particle concentration.

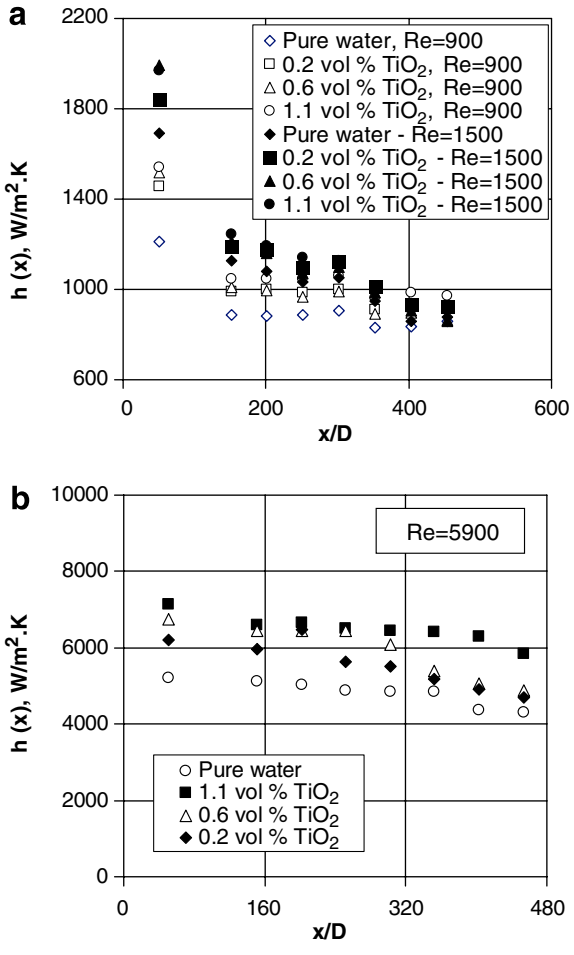

Fig. 6. Axial profiles of heat transfer coefficient at different particle concentrations (particle average diameter = 95 nm). (a) Laminar flows and (b) turbulent flows.

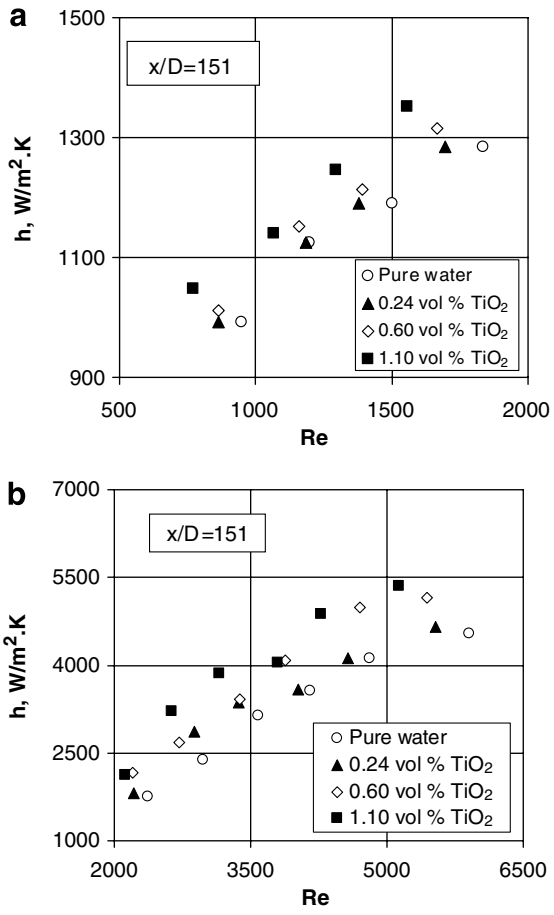

Fig. 7. Convective heat transfer coefficient as a function of Reynolds number with different particle concentrations ($x/D = 151$). (a) Laminar flows and (b) turbulent flows.

3.3.3. Effect of particle (agglomerate) size

Fig. 8 shows the convective heat transfer coefficient as a function of Reynolds number with different average particle sizes in the laminar flow regime. The average particle size is seen to have marginal effect under the conditions of this work although the thermal conductivity is found to decrease with increasing particle size (Fig. 3b). The results in the turbulent flow regime show a similar trend.

3.3.4. Further discussion of the experimental results

The observed effects of particle concentration and flow Reynolds number, and the unexpected marginal effect of particle size may be explained by the macroscopic theory for the forced convective heat transfer, which states that the convective heat transfer coefficient, h, can be

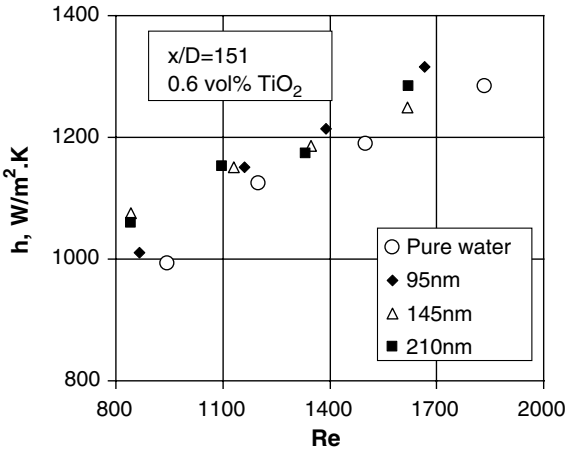

Fig. 8. Effect of particle size on the convective heat transfer coefficient.

approximately given by $h = k_f/\delta_t$ with δ_t the thickness of thermal boundary layer. The simple expression indicates that both an increase in k_f and a decrease in δ_t increase the convective heat transfer coefficient. It is not difficult to explain the positive effect of the Reynolds number on the convective heat transfer as an increase in the Reynolds number leads to a decrease in the boundary layer thickness and an increase in the thermal conduction due to the so-called dynamic effect [25]. The following discussion will therefore focus on the effects of particle concentration and size.

As clearly shown in Fig. 3, addition of nanoparticles enhances the thermal conduction and the enhancement increases with increasing particle concentration for a given particle size. The enhancement of the thermal conduction should increase the convective heat transfer coefficient. However, the increase in particle concentration also increases the fluid viscosity, which should result in an increase in the boundary layer thickness hence a decrease in the convective heat transfer coefficient. As shown clearly in Section 3.3.2, addition of nanoparticles enhances the convective heat transfer. This indicates that the positive effect of the thermal conduction enhancement outweighs the negative effect of the viscosity increase under the conditions of this work. Here the positive effect of thermal conduction enhancement should also include possible enhancement of thermal conduction due to the dynamic flow effect. Although no experimental data are available for the thermal conductivity enhancement due to the dynamic flow effect, previous work by Ahuja [1,2], Sohn and Chen [25] and Shin and Lee [24] clearly indicate that the thermal conductivity increases with increasing shear rate. Clearly, more work is needed to quantify this effect for nanofluids.

As discussed in Section 3.3.3, particle size only has a marginal effect on the convective heat transfer under the conditions of this work. This is unexpected because nanofluids containing larger particles have been shown in Sections 3.1 and 3.2 to have a lower thermal conductivity and a higher viscosity both of which should have led to a lower convective heat transfer coefficient. A possible reason for the unexpected result may be the particle migration mechanism [31]. According to such a mechanism, large particles tend to migrate to the central part of the pipe, which could lead to a particle depletion region with low viscosity at the wall hence a decrease in the boundary layer thickness. On the other hand, small particles tend to be uniformly distributed over the pipe cross-section due to the Brownian motion. This may imply that, for a given average particle concentration, the wall region could have a higher solids concentration hence a higher viscosity when the flowing nanofluids contain smaller particles. The combination of the above two opposite effects could have been responsible for the observed marginal effect of particle size under the conditions of this work. Clearly, the proposed particle migration mechanism is a hypothesis; further experimental verification is needed before a firm conclusion can be reached.

3.4. Pressure drop

The pressure drop of nanofluids flowing through the whole length of the copper tube was measured under various conditions. Fig. 9(a) and (b) shows the measured

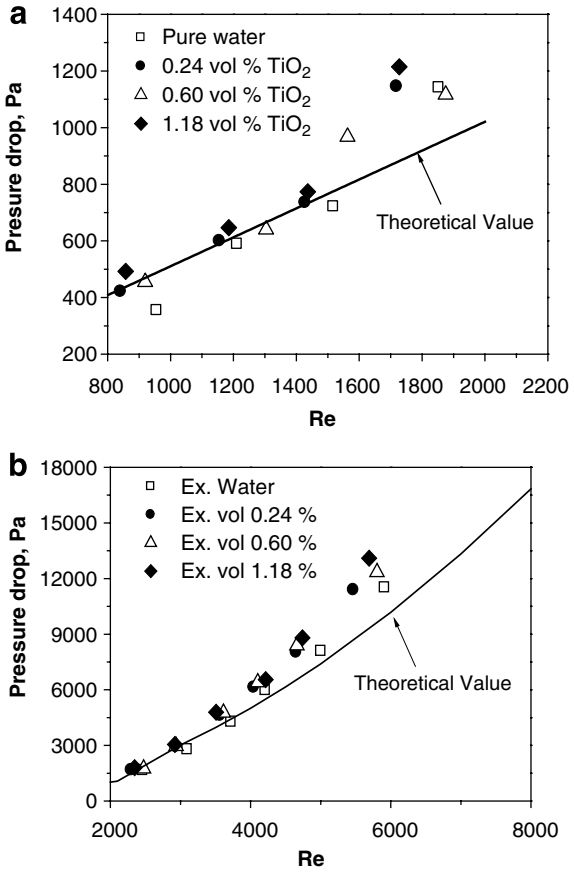

Fig. 9. Pressure drop as a function of Reynolds number (95 nm nanoparticles). (a) Laminar flows and (b) turbulent flows.

results together with predictions with the following expression:

$$\Delta p = \frac{2f\rho_f u^2 L}{D} \tag{7}$$

where Δp is the pressure drop which has taken the effect of gravity into account, L is the length of the copper test tube, and f is the friction factor. The frictional factor depends on the Reynolds number. In laminar flow regime ($Re < 2300$), the following Hagen–Poiseuille equation is used in the calculation (Fig. 9a):

$$f = 16/Re \tag{7a}$$

whereas Eq. (6a), the so-called Blasius equation, is used for the turbulent flow regime (Fig. 9b). In the laminar flow regime, predictions by Eqs. (7) and (7a) agree well with the measurements at $Re < \sim 1500$, but the equations underpredict the measurements at $Re > \sim 1500$ (Fig. 9a). Pressure drop in the turbulent regime is significantly higher than that in the laminar flow regime as shown in Fig. 9(b). Similar to the case in the laminar flow regime, predictions by Eqs. (7) and (7a) agree well with measurements at $Re = 2300$–4000, but the two equations underpredict the measurements at $Re > \sim 4000$. An inspection of Fig. 9(a) and (b) indicate that the pressure drop of nanofluids is very close to that of the base liquid for a given Reynolds number.

The deviation of Eq. (7) from the measurements in both the laminar and turbulent flow regimes at relatively high Reynolds numbers may be associated with the entrance effect, which is not included in Eq. (7) but included in the measurements as only two transducers were used in the experiments to avoid affecting the heat transfer experiments. For a Newtonian fluid flowing through a straight pipe, the flow is hydrodynamically fully developed at $x/D \geqslant \sim(0.05Re)$. For flows with a low Reynolds number, the entrance length is small hence its effect on the total pressure drop is small. The entrance length increases with increasing Reynolds number, and the effect of the entrance length could become considerable at high Reynolds numbers. It should be noted that the above explanation requires further experimental validation through for example measurements of pressure distribution in the entrance region using a test section exactly the same as the one used for the heat transfer work. Further work should also be done on analysis of the non-Newtonian behaviour of nanofluids which may shed light on the experimental observations. These are planned for our future work.

4. Concluding remarks

An experimental study has been carried out on the flow and heat transfer behaviour of aqueous TiO_2 nanofluids flowing through a straight vertical pipe under both the laminar and turbulent flow conditions. The effects of nanoparticles concentrations, particle (agglomerate) size, and the flow Reynolds number are investigated. The following conclusions are obtained:

- Addition of nanoparticles into the base liquid enhances the thermal conduction and the enhancement increases with increasing particle concentration and decreasing particle (agglomerate) size.
- Nanofluids used in this work show the shear thinning behaviour and the shear viscosity tends to be a constant at shear rates greater than $\sim 100\ s^{-1}$. The constant viscosity increases with increasing particle concentration and particle (agglomerate) size.
- Given the flow Reynolds number and particle size, the convective heat transfer coefficient increases with nanoparticle concentration in both the laminar and turbulent flow regimes and the effect of particle concentration seems to be more considerable in the turbulent flow regimes.
- Given the particle concentration and flow Reynolds number, the convective heat transfer coefficient does not seem to be sensitive to the average particle size under the conditions of this work. The small effect of particle size on the convective heat transfer coefficient could be due to particle migration.
- Pressure drop of nanofluids is very close to that of the base liquid given the flow Reynolds number. Predictions of the pressure drop with the conventional theory for the base liquid agree well with the measurements at relatively low Reynolds numbers. Deviation occurs at high Reynolds numbers possibly due to the entrance effect.

More work is clearly required to validate various explanations put forward for the marginal effect of particle size and deviation from the theory for the pressure drop at relatively high Reynolds numbers.

Acknowledgements

Y.D. and Y.H. would like to thank UK EPSRC for partial financial support under Grant EP/D000645/1. H.C. wishes to thank the Institute of Engineering Thermophysics of the Chinese Academy of Sciences for a visiting fellowship. Thanks are due to Dr. D. Wen of Queen Mary College of the University of London for various advices particularly the data requisition system.

References

[1] A.S. Ahuja, Augmentation of heat transport in laminar flow of polystyrene suspension: I – experiments and results, J. Appl. Phys. 46 (1975) 3408–3416.
[2] A.S. Ahuja, Augmentation of heat transport in laminar flow of polystyrene suspension: II – analysis of data, J. Appl. Phys. 46 (1975) 3417–3425.
[3] S.U.S. Choi, Enhancing thermal conductivity of fluids with nanoparticles, in: D.A. Siginer, H.P. Wang (Eds.), Developments Applications of Non-Newtonian Flows, FED-vol. 231/MD-vol. 66, ASME, New York, 1995, pp. 99–105.

[4] S.K. Das, N. Putra, W. Roetzel, Pool boiling characteristics of nano-fluids, Int. J. Heat Mass Transfer 46 (2003) 851–862.
[5] S.K. Das, N. Putra, W. Roetzel, Pool boiling of nano-fluids on horizontal narrow tubes, Int. J. Multiphase Flow 29 (2003) 1237–1247.
[6] S.K. Das, N. Putra, P. Thiesen, W. Roetzel, Temperature dependence of thermal conductivity enhancement for nanofluids, ASME J. Heat Transfer 125 (2003) 567–574.
[7] Y.L. Ding, H. Alias, D.S. Wen, R.A. Williams, Heat transfer of aqueous suspensions of carbon nanotubes (CNT nanofluids), Int. J. Heat Mass Transfer 49 (2006) 240–250.
[8] J.A.Eastman, S.U.S. Choi, S. Li, L.J. Thompson, S. Lee, Enhanced thermal conductivity through the development of nanofluids, in; 1996 Fall Meeting of the Materials Research Society (MRs), Boston, USA, 1996, pp. 3–11.
[9] J.A. Eastman, S.U.S. Choi, S. Li, W. Yu, L.J. Thompson, Anomalously increased effective thermal conductivities of ethylene glycol-based nanofluids containing copper nanoparticles, Appl. Phys. Lett. 78 (2001) 718–720.
[10] V. Gnielinski, New equations for heat and mass transfer in turbulent pipe and channel flow, Int. Chem. Eng. 16 (1976) 359–368.
[11] R.L. Hamilton, O.K. Crosser, Thermal conductivity of heterogeneous two-component systems, I&EC Fundam. 125 (3) (1962) 187–191.
[12] G. Hetsroni, R. Rozenblit, Heat transfer to a liquid–solid mixture in a flume, Int. J. Multiphase Flow 20 (1994) 671–689.
[13] Y.K. Hong, D.H. Eom, S.H. Lee, T.G. Kim, J.G. Park, A.A. Bushaina, The effect of additives in post-Cu CMP cleaning on particle adhesion and removal, J. Electrochem. Soc. 151 (2004) G756–G761.
[14] P. Keblinski, S.RE. Phillpot, S.U.S. Choi, J.A. Eastman, Mechanisms of heat flow in suspensions of nano-sized particles (nanofluids), Int. J. Heat Mass Transfer 45 (2002) 855–863.
[15] K. Khanafer, K. Vafai, M. Lightstone, Buoyancy-driven heat transfer enhancement in a two-dimensional enclosure utilizing nanofluids, Int. J. Heat Mass Transfer 46 (2003) 3639–3653.
[16] S. Lee, S.U.S. Choi, Application of metallic nanoparticle suspensions in advanced cooling systems, in: 1996 International Mechanical Engineering Congress and Exhibition, Atlanta, USA, 1996.
[17] S. Lee, S.U.S. Choi, S. Li, J.A. Eastman, Measuring thermal conductivity of fluids containing oxide nanoparticles, J. Heat Transfer, Trans. ASME 121 (1999) 280–289.
[18] D. Lee, J.W. Kim, B.G. Kim, A new parameter to control heat transport in nanofluids: surface charge state of the particle in suspension, J. Phys. Chem. B 110 (2006) 4323–4328.
[19] Q. Li, Y.M. Xuan, Convective heat transfer and flow characteristics of Cu-water nanofluids, Sci. China, Ser. E 45 (2002) 408–416.
[20] H. Masuda, A. Ebata, K. Teramae, N. Hishiunma, Alteration of thermal conductivity and viscosity of liquid by dispersed by ultra-fine particles (dispersion of γ-Al_2O_3, SiO_2 and TiO_2 ultra-fine particles), Netsu Bussei (Japan) 4 (1993) 227–233.
[21] S.M.S. Murshed, K.C. Leong, C. Yang, Enhanced thermal conductivity of TiO_2-water based nanofluids, Int. J. Therm. Sci. 44 (2005) 367–373.
[22] B.C. Pak, Y.I. Cho, Hydrodynamic and heat transfer study of dispersed fluids with submicron metallic oxide particles, Exp. Heat Transfer 11 (1998) 150–170.
[23] R.K. Shah, Thermal entry length solutions for the circular tube and parallel plates, in: Proceedings of the 3rd National Heat and Mass Transfer Conference, Indian Institute of Technology, Bombay, 1975, I (Paper HMT-11-75).
[24] S. Shin, S. Lee, Thermal conductivity of suspensions in shear flow fields, Int. J. Heat Mass Transfer 43 (2000) 4275–4284.
[25] C.W. Sohn, M.M. Chen, Microconvective thermal conductivity in disperse two phase mixture as observed in a low velocity Couette flow experiment, J. Heat Transfer, Trans. ASME 103 (1981) 47–51.
[26] P. Vassallo, R. Kumar, S. Damico, Pool boiling heat transfer experiments in silica-water nano-fluids, Int. J. Heat Mass Transfer 47 (2004) 407–411.
[27] X.W. Wang, X.F. Xu, S.U.S. Choi, Thermal conductivity of nanoparticle–fluid mixture, J. Thermophys. Heat Transfer 13 (1999) 474–480.
[28] D.S. Wen, Y.L. Ding, Effective thermal conductivity of aqueous suspensions of carbon nanotubes (nanofluids), J. Thermophys. Heat Transfer 18 (4) (2004) 481–485.
[29] D.S. Wen, Y.L. Ding, Experiment investigation into convective heat transfer of nanofluids at the entrance region under laminar flow conditions, Int. J. Heat Mass Transfer 47 (2004) 5181–5188.
[30] D.S. Wen, Y.L. Ding, Experimental investigation into the pool boiling heat transfer of aqueous based γ-alumina nanofluids, J. Nanopart. Res. 7 (2005) 265–274.
[31] D.S. Wen, Y.L. Ding, Effect on heat transfer of particle migration in suspensions of nanoparticles flowing through minichannels, Microfluid. Nanofluid. 1 (2) (2005) 183–189.
[32] H. Xie, J. Wang, T.G. Xi, Y. Liu, F. Ai, Thermal conductivity enhancement of suspensions containing nanosized alumina particles, J. Appl. Phys. 91 (2002) 4568–4572.
[33] Y.M. Xuan, W. Roetzel, Conceptions for heat transfer correlation of nanofluids, Int. J. Heat Mass Transfer 43 (2000) 3701–3707.
[34] Y.M. Xuan, Q. Li, Heat transfer enhancement of nanofluids, Int. J. Heat Fluid Flow 21 (2000) 58–64.
[35] Y.M. Xuan, Q. Li, Investigation on convective heat transfer and flow features of nanofluids, J. Heat transfer, ASME 125 (2003) 151–155s.
[36] Y.M. Xuan, Q. Li, W.F. Hu, Aggregation structure and thermal conductivity of nanofluids, Thermodynamics, AIChE J. 49 (4) (2003) 1038–1043.
[37] Y. Yang, Z.G. Zhong, E.A. Grulke, W.B. Anderson, G. Wu, Heat transfer properties of nanoparticle-in-fluid dispersion (nanofluids) in laminar flow, Int. J. Heat Mass Transfer 48 (2005) 1107–1116.
[38] S.M. You, J.H. Kim, K.H. Kim, Effect of nanoparticles on critical heat flux of water in pool boiling heat transfer, Appl. Phys. Lett. 83 (2003) 3374–3376.